Int. J. Heat Mass Transfer. Vol. 22, pp. 909–917

0017-9310/79/0601-0909 $02.00/0

THE EFFECT OF A MIXING TEE ON TURBULENT HEAT TRANSFER IN A TUBE

E. M. SPARROW and R. G. KEMINK
Department of Mechanical Engineering, University of Minnesota, Minneapolis, MN 55455, U.S.A.

(*Received* 6 *September* 1978 *and in revised form* 1 *November* 1978)

Abstract—Heat-transfer coefficients for turbulent airflow in a circular tube situated downstream of a mixing tee have been determined experimentally. In the experiments, perpendicularly oriented air streams were respectively ducted to a tee via its center port and a side port. The merged flow exited the tee from the other side port and passed into the heated test section tube. From the experimental data, results were obtained for the circumferential average heat-transfer coefficient at a succession of axial stations and for the circumferential variation of the transfer coefficient at each such station. It was found that the mixing and turning of the flow gives rise to a substantial augmentation of the heat-transfer coefficients compared with those in a conventional thermal entrance region; the thermal entrance length is also substantially elongated. At a given Reynolds number, the axial distributions of the circumferential average coefficient are bounded between the distributions for the two limiting cases of no mixing (i.e. entire flow entering either via the side port or via the center port). When the axial distributions are normalized by the corresponding fully developed values, they are nearly insensitive to the Reynolds number. The circumferential variations are largest just downstream of the tee. In most cases, the variations decay to the $\pm 3\%$ level at 12 diameters downstream of the tee, but in some instances residual variations persist at 40–60 diameters.

NOMENCLATURE

c_p, specific heat at constant pressure;
D, diameter of tube bore;
$\bar{h}_x$, circumferential average heat-transfer coefficient at x;
$h_x(\theta)$, local heat-transfer coefficient at x, θ;
k, thermal conductivity of air;
k_w, thermal conductivity of tube wall;
$\dot{m}$, mass flow rate in test section;
$\dot{m}_1$, mass flow rate entering via side port, Fig. 1;
$\dot{m}_2$, mass flow rate entering via center port, Fig. 1;
$\overline{Nu}_{fd}$, fully developed Nusselt number;
$\overline{Nu}_x$, circumferential average Nusselt number at x;
$Nu_x(\theta)$, local Nusselt number at x, θ;
$\bar{q}_x$, circumferential average heat flux at x;
$q_x(\theta)$, local heat flux at x, θ;
Re, test section Reynolds number;
R_i, inner radius of tube, $D/2$;
R_m, mean radius of tube wall;
T_{bo}, bulk temperature of fluid entering tee;
T_{bx}, local bulk temperature at x;
$\overline{T}_{wx}$, circumferential average wall temperature at x;
$T_{wx}(\theta)$, local wall temperature at x, θ;
T_∞, temperature of surroundings;
t, tube wall thickness;
x, axial coordinate, Fig. 1;
x_e, thermal entrance length;
θ, angular coordinate;
μ, viscosity.

INTRODUCTION

THE MIXING of two pipe flows that intersect at right angles causes major hydrodynamic disturbances and dislocations which may persist in the merged flow in the pipeline downstream of the point of mixing. It is logical to expect that the decaying disturbances and the flow redevelopment that occurs in response to the dislocations will significantly affect the heat transfer in the downstream pipeline. In view of this expectation and of the fact that mixing tees are commonly encountered in piping systems, it is noteworthy that the literature appears void of studies of the heat-transfer ramifications of pipeline mixing. The present research was undertaken to experimentally determine the heat-transfer characteristics for turbulent flow in a circular tube situated downstream of a mixing tee.

In the experiments, air was delivered to the center port and to one of the side ports of a tee. Upon mixing, the merged flow exited the tee through the other side port and passed into an electrically heated circular tube. The tube was heavily instrumented to enable determination of both the circumferential variation of the heat-transfer coefficient at a succession of axial stations and the circumferential average coefficient at each station.

A schematic diagram showing the mixing arrangement is presented in the inset at the upper right of Fig. 1. As indicated there, the mass flows of the entering streams are denoted by $\dot{m}_1$ and $\dot{m}_2$, respectively for the side port and the center port; the mass flow in the downstream tube is denoted by $\dot{m}$ $(=\dot{m}_1+\dot{m}_2)$. Both entering streams are at the same

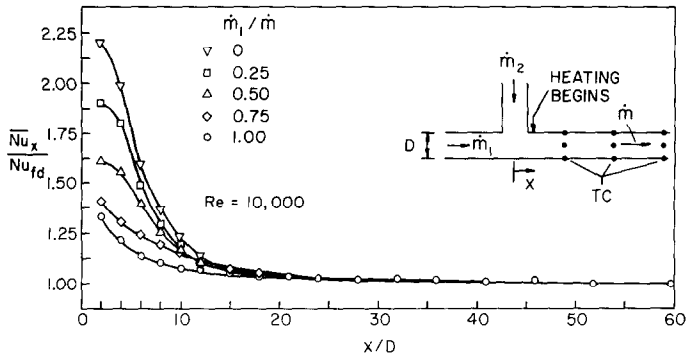

FIG. 1. Circumferential average Nusselt numbers for $Re = 10000$ and for various mixing proportions. Inset shows schematic of the mixing arrangement.

temperature. Heating begins immediately downstream of the tee, as does the array of thermocouples (identified in the diagram as TC) deployed both around and along the tube wall.

The experiments were performed with a view to identifying how the heat-transfer coefficients for a test section flow of fixed Reynolds number Re respond to differences in the proportions of the two entering streams. Thus, at a given Re, experiments were carried out for the two limiting cases of no mixing, respectively $\dot{m}_1 = \dot{m}$ ($\dot{m}_2 = 0$) and $\dot{m}_2 = \dot{m}$ ($\dot{m}_1 = 0$) and for various degrees of mixing characterized by the ratio $\dot{m}_1/\dot{m}$. The fixed test section Reynolds numbers employed in the experiments were 10000, 20000 and 30000 and, for each of these, the $\dot{m}_1/\dot{m}$ ratio was given values of 0, 0.25, 0.5, 0.75 and 1.

In the presentation of the results, the circumferential average Nusselt numbers are viewed from two different perspectives. In one, the axial distributions corresponding to the various $\dot{m}_1/\dot{m}$ values at a fixed Reynolds number are brought together and compared. This presentation illuminates the influence of the upstream history of the flow (i.e. the proportions of the component flows) on the test section Nusselt numbers. Of particular interest in this presentation is the role of the limiting cases $\dot{m}_1/\dot{m} = 0$ and $\dot{m}_1/\dot{m} = 1$ as brackets on the results for the cases where mixing occurs. A second viewpoint is projected by fixing the $\dot{m}_1/\dot{m}$ ratio and examining the effect of the Reynolds number on the Nusselt number distributions. The aim of this presentation is to demonstrate that the axial distributions of the Nusselt number, when normalized by the corresponding fully developed Nusselt number, are insensitive to the Reynolds number for a fixed value of $\dot{m}_1/\dot{m}$.

The circumferential average Nusselt number results are also employed to identify the length of the thermal entrance region. For this purpose, the entrance length is defined in terms of the axial station at which the circumferential average Nusselt number differs by 5% from the corresponding fully developed value.

The turning of the flow at the tee produces circumferential variations of the Nusselt number. The circumferential distributions are presented at a succession of axial stations to document the pattern of their decay. The effect of the upstream history of the flow on the circumferential variations is displayed via comparisons of the results for various $\dot{m}_1/\dot{m}$ ratios.

As indicated earlier, there appear to be no published results of the type sought in the present investigation, so that comparisons with the literature are not possible.

EXPERIMENTAL APPARATUS

The two pipe flows that participated in the mixing process were both supplied from a central dryer-equipped air compressor and were, therefore, at the same temperature. Each of the flows was ducted through a 100-diameters-long hydrodynamic development tube prior to being delivered, respectively, to the center port and one of the side ports of a tee. The other side port, which served as the exit for the merged flow, mated with the 100-diameters-long test section tube. After traversing the length of the heated test section, the air was discharged outside of the laboratory room. The operation of the system was, therefore, in the open circuit mode.

As set up for the experiments, the test section tube and the hydrodynamic development tube supplying the side port of the tee were colinear and horizontal. The development tube supplying the center port was vertical. Special care was taken to ensure that the two development tubes were at right angles to each other. All three tubes were cut from a single length of type 304 stainless steel tubing. They were internally honed to a high degree of smoothness and subsequently straightened by a technique employed for straightening the barrels of firearms. The inside diameter, after honing, was 2.37 cm (0.933 in).

Since the heating of the test section tube was to be accomplished by ohmic dissipation within the tube wall, it was necessary to know the wall thickness. For this purpose, the thickness of short lengths of tubing cut from the ends of the respective tubes was measured both by a specially fitted micrometer and by an optical comparator. Both measurements revealed the presence of a small but regular circum-

ferential variation which was the same for all of the available samples. This variation was well represented by

$$t = 0.0894 - 0.00559\cos\theta, \quad (1)$$

where t is the wall thickness in cm and θ is the angular coordinate. This thickness variation was taken into account in the data reduction.

The electric current for the ohmic heating was passed into and out of the test section via specially designed bus bars attached to the respective ends of the tube. Owing to the relatively low resistance of the test section tube ($\sim 0.024\,\Omega$), it was necessary to design for fairly high currents (up to 100 A). In order to avoid obliterating any circumferential temperature variations which would otherwise exist in the tube, the conventional arrangement consisting of a tube-girdling copper (or aluminum) ring fed by a single large cable was not used. Instead, a ring made up of twelve individual circumferential segments was employed. Electric current was carried to (or from) each segment by a 0.32 cm (1/8 in) dia radially oriented copper rod. The outer ends of the rods terminated in a large circular copper strap to which the main current cables were connected.

Out of concern for radial heat losses at the entrance of the test section, each of the current-carrying rods was fitted with a guard heater and a differential thermocouple, and the entire bus bar assembly was embedded in silica aerogel insulation. The guard heater arrangement performed its function satisfactorily at test section Reynolds numbers up to 30 000, but beyond that it was not possible to null out the radial heat flow in all of the rods. For this reason, final data runs were not made for Reynolds numbers above 30 000. For the downstream bus bar assembly, which was 10 diameters from the nearest measurement station, it was deemed sufficient to embed it in insulation consisting of the aerogel powder packed between sheets of fiberglass.

Outside surface temperatures were measured around the circumference and along the length of the test section tube with calibrated 36-gage iron and constantan thermocouples. The axial positions of the thermocouples are expressed by the x coordinate which, as shown in the inset of Fig. 1, is measured from the center of the tee, and the first set of thermocouples is at $x/D = 2$ (D = inside diameter of tube). The circumferential position is specified by the angle θ, where $\theta = 0°$ corresponds to the top of the tube and $\theta = 180°$ to the bottom. At each of seventeen axial stations between $x/D = 2$ and 60, eight thermocouples were distributed uniformly around the circumference at 45° intervals. The locations of these thermocouples will be evident from the presentation of results. At $x/D = 70$, 80 and 90, there were two thermocouples, respectively positioned at $\theta = 0°$ and 180°.

The tee itself was fabricated by modifying one that was commercially available. To avoid spurious heat conduction which would give rise to uncertainties in the thermal boundary conditions, a thin-walled, nonmetallic tee made of chlorinated polyvinyl chloride (cpvc) was employed. The wall thickness of the tee was reduced to the minimum consistent with structural integrity and the inside diameter was finished bored to the internal diameters of the stainless steel tubes. Furthermore, the axial length of the tee was shortened to enable the heated test section tube to be placed as close as possible to the center port. This was done to minimize possible ambiguities associated with the redevelopment of the velocity field prior to the onset of heating. The axial distance from the center of the tee to the start of heating was 0.76 diameters, as indicated in Fig. 1.

The mass flow rates $\dot{m}_1$ and $\dot{m}_2$ of the two pipe flows that participated in the mixing process were measured with calibrated rotameters positioned upstream of the respective hydrodynamic development tubes. The effectiveness of the pressure regulator used to damp out line fluctuations was clearly evidenced by the fact that no oscillations of the rotameter floats could be observed. The bulk temperature at the inlet of each of the development tubes was measured by a thermocouple rake.

The test section and hydrodynamic development tubes were each housed in a 30 cm (12 in) square plywood box whose function was to contain insulation. Two different insulations were used: silica aerogel and fiberglass. Of these, silica aerogel is the better (thermal conductivity less than air), but its exclusive use would have been prohibitively expensive. The aerogel, being a powder, was poured into the space adjacent to the tubes and was also used exclusively in the neighborhood of the tee. The fiberglass was positioned so as to form a casing around the aerogel.

DATA REDUCTION

The two types of heat-transfer coefficients that were evaluated from the data are the local coefficient $h_x(\theta)$ at x,θ and the circumferential average coefficient $\bar{h}_x$ corresponding to an axial station x. These coefficients are defined as

$$h_x(\theta) = \frac{q_x(\theta)}{T_{wx}(\theta) - T_{bx}}, \quad \bar{h}_x = \frac{\bar{q}_x}{\bar{T}_{wx} - T_{bx}}. \quad (2)$$

The heat fluxes $q_x(\theta)$ and $\bar{q}_x$ respectively represent local and circumferential average values and the wall temperatures $T_{wx}(\theta)$ and $\bar{T}_{wx}$ have corresponding meanings. Since the wall temperatures in equation (2) correspond to those on the inside surface of the tube, a small calculated correction (~ 0.01°C) was applied to the measured outside wall temperatures. The heat fluxes are also based on the inside wall area and the quantity T_{bx} is the bulk temperature at axial station x.

For the evaluation of $\bar{h}_x$, the average heat flux $\bar{q}_x$ was determined from the input power P, the tube inside wall area πDL (D = inside diameter, L = length) and the heat loss $\bar{q}_{lx}$, so that

$$\bar{q}_x = P/\pi DL - \bar{q}_{lx}. \quad (3)$$

The heat loss $\bar{q}_{lx}$ was evaluated along a radial flow path between the outside wall of the tube and the surroundings, with $(\overline{T}_{wx}-T_\infty)$ as the participating temperature difference. The flow path included the series resistances of the insulation and the natural convection external to the plywood enclosure that housed the insulation. Axial conduction in the tube wall was found to be of no significance.

The circumferential average wall temperature $\overline{T}_{wx}$ was taken as the average of the eight temperatures measured at equally spaced angular positions at x. For the bulk temperature, the differential fluid energy balance $\mathrm{d}T_b/\mathrm{d}x = \bar{q}_x \pi D/\dot{m}c_p$ was integrated to yield

$$T_{bx} = T_{bo} + (\pi D/\dot{m}c_p)\int_0^x \bar{q}_x \,\mathrm{d}x. \tag{4}$$

Since $\bar{q}_x$ is a function of x (owing to the variation of $\bar{q}_{lx}$ with x), the indicated integration was performed numerically. The quantity T_{bo} is the bulk temperature of the fluid entering the tee.

For the evaluation of the local heat-transfer coefficient $h_x(\theta)$ from equation (2), the key input that is needed is the local heat flux $q_x(\theta)$ at position x,θ. To determine this quantity, an energy balance is written for a volume element of dimensions t by $R_m\,\mathrm{d}\theta$ by $\mathrm{d}x$ which spans the thickness t of the tube wall and subtends an arc $R_m\,\mathrm{d}\theta$ (R_m = mean radius of tube wall). The use of such a wall-spanning control volume is admissible because of the extremely small radial temperature change. Correspondingly, at any axial station x, T_{wx} is a function only of θ. It was found that the measured circumferential temperature variations could be very well fitted by the representation

$$T_{wx}(\theta) = \overline{T}_{wx} + a_1 \cos\theta, \tag{5}$$

where

$$a_1 = (\tfrac{1}{4})\sum_{j=1}^{8} T_{wx}(\theta_j)\cos\theta_j \tag{6}$$

and $\theta_j = (j-1)\pi/4$. The representation (5) was employed in evaluating the first and second derivatives, $\partial T_{wx}/\partial\theta$ and $\partial^2 T_{wx}/\partial\theta^2$ respectively, that are needed for the energy balance.

For the energy balance, the relevant terms include: (a) $q_x(\theta)$, (b) the ohmic dissipation, (c) the net circumferential heat inflow, and (d) the heat loss from the outside surface of the tube. Mathematically, the balance can be written as

$$q_x(\theta) = (R_m t/R_i)P''' + \frac{k_w}{R_i}\frac{\partial}{\partial\theta}\left[\frac{t}{R_m}\frac{\partial T_{wx}}{\partial\theta}\right] - q_{lx}(\theta), \tag{7}$$

where P''' is the volumetric heating rate, R_i is the inner radius of the wall ($= D/2$) and R_m, the mean radius, is equal to $R_i + t/2$. From measurements, it was found that R_i was very nearly independent of the θ and, with this, the $\partial/\partial\theta$ term can be expanded as

$$\frac{t}{R_m}\frac{\partial^2 T_{wx}}{\partial\theta^2} + \frac{1}{R_m}\frac{\partial T_{wx}}{\partial\theta}\frac{\partial t}{\partial\theta}\left[1 - \frac{t}{2R_m}\right] \tag{8}$$

In view of the algebraic fits to t and T_{wx}, equations (1) and (5) respectively, all of the derivatives were available in algebraic form. Of the two terms appearing in equation (8), the first was strongly dominant.

The last term of equation (7) is based on the series resistances of the insulation and the external natural convection together with the temperature difference $[T_{wx}(\theta)-T_\infty]$. With $q_x(\theta)$ from equation (7), T_{bx} from equation (4) and the measured value of $T_{wx}(\theta)$, all of the ingredients for the local coefficient $h_x(\theta)$ were available.

Dimensionless representation of $\bar{h}_x$ and $h_x(\theta)$ is made via the Nusselt numbers

$$\overline{Nu}_x = \bar{h}_x D/k, \quad Nu_x(\theta) = h_x(\theta)D/k, \tag{9}$$

in which k is the thermal conductivity of air at the bulk temperature T_{bx}. At sufficiently large downstream distances, where $\overline{Nu}_x$ becomes independent of x, it will be denoted by Nu_{fd} ($fd \sim$ fully developed). The test section Reynolds number Re was evaluated from

$$Re = 4\dot{m}/\mu\pi D, \tag{10}$$

where $\dot{m}$ is the sum of the measured component flow rates $\dot{m}_1$ and $\dot{m}_2$ and μ is the viscosity of air at the mean bulk temperature. The Prandtl number for all the experiments was approximately 0.7.

Variable property effects did not play a major role since the inlet-to-exit bulk temperature rise was only about 11°C (20°F). Furthermore, the largest wall-to-bulk temperature difference was about 7°C (12°F).

RESULTS AND DISCUSSION

Circumferential average results

The presentation of results will focus first on the circumferential average Nusselt numbers and Figs. 1 and 2 have been prepared to convey this information. In each figure, the circumferential average Nusselt number $\overline{Nu}_x$ at x is ratioed with the corresponding fully developed value Nu_{fd} (at the same Reynolds number) and plotted as a function of the dimensionless axial coordinate x/D. Figure 1 gives the $Re = 10\,000$ results, while Fig. 2 contains two graphs, respectively for $Re = 20\,000$ and $30\,000$. The data that appear in each figure are parameterized by the $\dot{m}_1/\dot{m}$ ratio, which ranges from zero to one. Curves have been faired through the data to provide continuity. The inset at the upper right of Fig. 1 serves to indicate that the x coordinate is measured from the center of the tee and that the heating begins at $x/D = 0.76$.

To provide perspective for the results of Figs. 1 and 2, note should be taken of the limiting cases $\dot{m}_1/\dot{m} = 0$ and 1 which correspond to situations where only one stream enters the tee. The case $\dot{m}_1/\dot{m} = 1$ corresponds to a straight throughflow in a constant area pipe although, as discussed shortly, the fluid experiences a disturbance as it encounters the aperture at the center port of the tee. In the other limit, $\dot{m}_1/\dot{m} = 0$, all the flow enters the tee via the

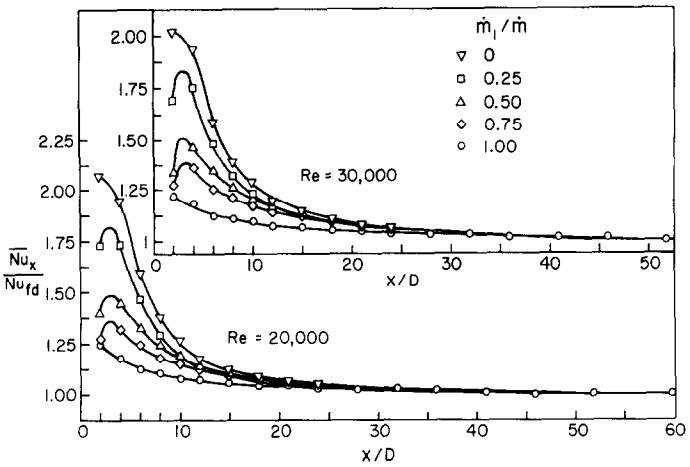

FIG. 2. Circumferential average Nusselt numbers for $Re = 20000$ and 30000 and for various mixing proportions.

central port and impinges with full force on the bottom of the tee before it turns and streams into the test section tube. Considering these two flow configurations, it can be concluded that $\dot{m}_1/\dot{m} = 1$ corresponds to a relatively placid hydrodynamic situation while $\dot{m}_1/\dot{m} = 0$ corresponds to a highly disturbed hydrodynamic situation. Consequently, the heat-transfer coefficients for the latter should be higher than those for the former.

With this as background, consideration may be given to the results of Figs. 1 and 2. From an overall inspection of the figures, it appears that not only do the $\dot{m}_1/\dot{m} = 0$ results lie above those for $\dot{m}_1/\dot{m} = 1$, but also that these cases are, respectively, upper and lower bounds for the mixing cases $0 < \dot{m}_1/\dot{m} < 1$. Furthermore, a first glance suggests that the results are arranged in a regular order with $\dot{m}_1/\dot{m}$, starting with the lowest coefficients when $\dot{m}_1/\dot{m} = 1$ and increasing monotonically to higher coefficients as $\dot{m}_1/\dot{m}$ decreases. From a closer inspection, it is seen that these characteristics hold without exception in a significant portion of the thermal entrance region, up to about $x/D = 10$. Practically speaking, this is the important part of the entrance region because it is there that the $\overline{Nu}_x/Nu_{fd}$ values are highest and the effects of $\dot{m}_1/\dot{m}$ are greatest (i.e. the curves are most spread). Thus, for practical purposes, the bounding and the monotonic ordering can be regarded as truly characteristic of the results.

For $x/D > \sim 10$, some crossing of the curves can be seen, but the crossing also tends toward a merging. In the case of $Re = 10000$, the $\dot{m}_1/\dot{m} = 0$ curve ceases to be an upper bound for $x/D > \sim 14$, but in this range of x/D the overall spread of the data with $\dot{m}_1/\dot{m}$ is small. Thus, the departures from the characteristics identified in the preceding paragraphs are not major.

In common with the thermal entrance region of conventional pipe flows, the highest heat-transfer coefficients of Figs. 1 and 2 occur adjacent to the beginning of the heated section, and the coefficients approach the fully developed value at large x/D. There are, however, numerous major differences between the results for the mixing-affected flow and those for conventional pipe flows. One of the main differences is in the magnitude of the heat-transfer coefficients. Those for a conventional pipe flow are closely approximated by the $\dot{m}_1/\dot{m} = 1$ distribution curves shown in Figs. 1 and 2. By comparing the other distribution curves in each graph with that for $\dot{m}_1/\dot{m} = 1$, it is clear that the turning and mixing processes lead to substantial augmentation of the heat-transfer coefficients in the entrance region.

The shape of the distribution curves is also affected by the turning and mixing. For a conventional thermal entrance region, the shape of the distribution is similar to that of the $\dot{m}_1/\dot{m} = 1$ curves, that is, a monotonic decrease with concave upward curvature. On the other hand, the distributions for $\dot{m}_1/\dot{m} \neq 1$ are inflected and some display local maxima, thereby testifying to the complexity of the flow. It is interesting to note that no local maxima are in evidence when $\dot{m}_1/\dot{m} = 0$, that is, when all the flow enters through the center port. Thus, it appears that the interaction of the two flows is a prerequisite for the existence of the maxima.

By way of explaining the local maxima, it may be conjectured that they are somehow related to (a) reattachment downstream of flow separation and/or (b) jet impingement. For cases where $\dot{m}_2 > 0$, (i.e. $\dot{m}_1/\dot{m} \neq 1$), it is reasonable to expect that the turning of the flow which enters the tee via the center port gives rise to a separation bubble situated in the upper part of the tee, just downstream of the center port. Similarly, the center-port flow possesses a jet-like character as it passes into the tee. The effect of the horizontal flow (i.e. the $\dot{m}_1$ flow) is to cause the separation bubble and its reattachment point to move downstream, and similarly for the impingement region of the jet. This downstream movement could account for the local maxima in evidence in Fig. 2. Local maxima are not in evidence in Fig. 1, that is, for $Re = 10000$, because they probably occur upstream of the first measurement station.

Before leaving Figs. 1 and 2, it is relevant to discuss the relationship between the results for the $\dot{m}_1/\dot{m} = 1$ case and those for the thermal entrance region of a conventional hydrodynamically developed pipe flow. A comparison with available literature information for the latter [1, 2] (not shown here to avoid confusion in Figs. 1 and 2) indicates rather close agreement, with the present results lying slightly high (by no more than 5%) in most of the thermal entrance region. Therefore, the flow disturbance caused by the aperture in the wall of the tee, i.e. at the center port, does not have a significant effect on the circumferential average heat-transfer coefficient.

The experimentally determined fully developed Nusselt numbers were compared with those given by the Petukhov–Popov correlation [3]. Agreement in all cases was to within 3% or better.

Thermal entrance lengths can be determined from distribution curves such as those of Figs. 1 and 2, but replotted with an ordinate scale which enables better resolution in the region near $\overline{Nu}_x/Nu_{fd} \sim 1$. As noted earlier, the thermal entrance length x_e will be defined as the axial station at which $\overline{Nu}_x/Nu_{fd} = 1.05$. The thus-determined entrance lengths are plotted in Fig. 4 as a function of the $\dot{m}_1/\dot{m}$ ratio, with the Reynolds number as a parameter. From an overview of the figure, it is seen that the entrance

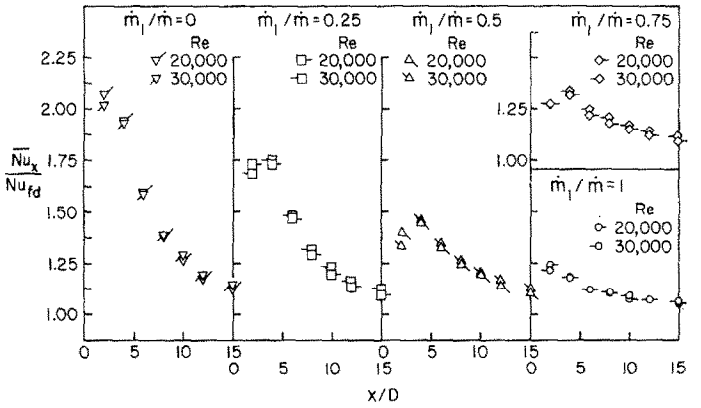

FIG. 3. Effect of Reynolds number on the circumferential average Nusselt number at various fixed mixing proportions.

An alternate presentation of the $\overline{Nu}_x$ results will now be made which highlights the effect of Reynolds number changes at various fixed values of $\dot{m}_1/\dot{m}$. This presentation is motivated by an observation which may be made in Fig. 2, namely, that the $\overline{Nu}_x/Nu_{fd}$ distribution curves for $Re = 20\,000$ and $30\,000$ are qualitatively similar. It is of interest to explore whether the similarity is more than qualitative and Fig. 3 has been prepared in this connection. Since the $Re = 10\,000$ distribution curves (Fig. 1) do not possess qualitative similarity with the others, they have not been included in Fig. 3.

Figure 3 is made up of five graphs, each of which pertains to a fixed value of $\dot{m}_1/\dot{m}$. In each graph, $\overline{Nu}_x/Nu_{fd}$ data for $Re = 20\,000$ and $30\,000$ are plotted as a function of x/D in the range between 2 and 15.

The figure shows that the data for the two Reynolds numbers are very nearly coincident. The largest deviations occur at the first measurement station for small and intermediate $\dot{m}_1/\dot{m}$, but these deviations are moderate. On the basis of this insensitivity to Reynolds number, it appears reasonable to employ the $Re = 30\,000$ $\overline{Nu}_x/Nu_{fd}$ curves of Fig. 2 for higher values of the Reynolds number. Thus, the results obtained here may be regarded as having a generality which extends beyond the actual Reynolds number range of the experiments.

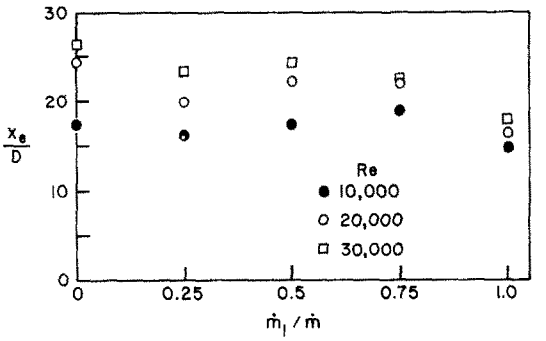

FIG. 4. Thermal entrance lengths based on $\overline{Nu}_x/Nu_{fd} = 1.05$.

lengths lie in the range from 15 to 25 diameters. This is to be contrasted with the 8–10 diameter entrance lengths for conventional turbulent airflows. Thus, the downstream region of heat transfer augmentation associated with the tee is substantially larger than the conventional thermal entrance region.

The entrance lengths for $Re = 10\,000$ are somewhat shorter than those for $Re = 20\,000$ and $30\,000$, which tend to group together. There is no clear trend with $\dot{m}_1/\dot{m}$, but the entrance lengths for the $\dot{m}_1/\dot{m} = 1$ case are generally lower than the others. On the other hand, the entrance lengths for this case are substantially larger than the conventional 8–10 diameter entrance lengths. To rationalize this differ-

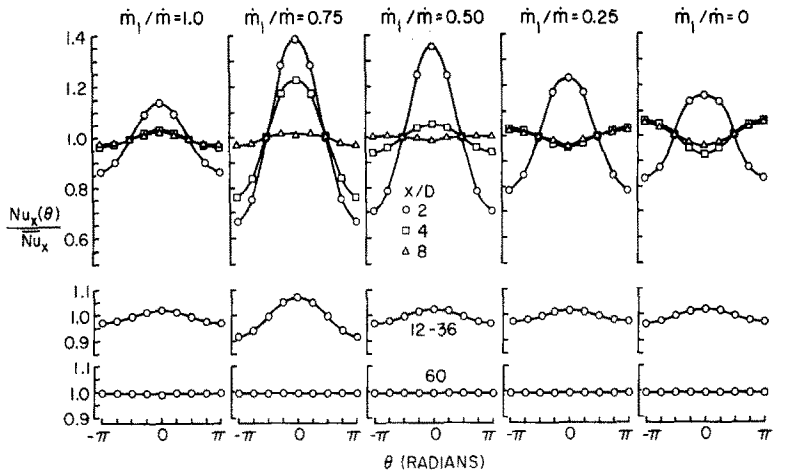

FIG. 5. Circumferential distributions of the Nusselt number, $Re = 10000$.

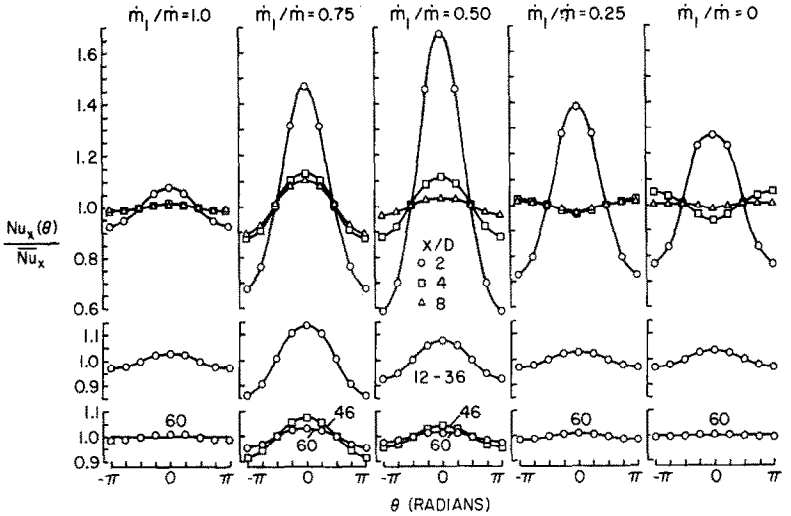

FIG. 6. Circumferential distributions of the Nusselt number, $Re = 30000$.

ence, it may be noted (as stated earlier) that the present values of $\overline{Nu_x}/Nu_{fd}$ lie slightly above the conventional values owing to the disturbance caused by the interrupted wall of the tee. Because of the flatness of the $\overline{Nu_x}/Nu_{fd}$ vs x/D curves as $\overline{Nu_x} \rightarrow Nu_{fd}$, the small deviation (a few per cent) can cause a relatively large shift in the entrance length.

There is some scatter in evidence in Fig. 4. The scatter is due to the uncertainties of graphical interpolation in the flat portions of the $\overline{Nu_x}/Nu_{fd}$ curves.

Circumferential variations

The complex fluid flow processes associated with the mixing and turning give rise to circumferential variations of the heat-transfer coefficient. The fluid which enters the tee via the center port possesses downward momentum which tends to concentrate the flow along the bottom wall of the tee. In addition, the inability of the center-port flow to abruptly change direction (from vertical downward to horizontal) causes a separation bubble to be formed near the upper wall of the tee. It is these two factors, the bottom-wall flow concentration and the top-wall separation bubble, that play the key roles in creating the circumferential fluid flows which cause the variations of the heat-transfer coefficient.

As the fluid streams into the test section from the tee, the initial flow concentration at the bottom wall tends to relieve itself by means of an upward circumferential motion along the sides of the tube. There are, in fact, two such upflowing streams, respectively along the wall of each vertical half of the tube. Each such stream can be regarded as a wall jet. The two wall jets tend to collide and merge just downstream of the separation bubble. It is well established that flow reattachment downstream of a separation bubble and collision of wall jets both give rise to high local heat-transfer coefficients.

With this as background, attention may be turned to the measured angular distributions of the heat-transfer coefficient and Figs. 5 and 6 have been prepared to convey this information. Each figure contains five panels which, successively, present results for $\dot{m}_1/\dot{m} = 1$, 0.75, 0.5, 0.25 and 0. In each

panel, the ratio $Nu_x(\theta)/\overline{Nu}_x$ is plotted as a function of the angular coordinate θ. These angular distributions are given for the various axial stations for which the x/D values are indicated in the graphs. Figures 5 and 6 correspond respectively to $Re = 10000$ and 30000—the lowest and highest of the Reynolds numbers. For the interpretation of the results, it should be noted that $\theta = 0°$ corresponds to the top of the tube and $\theta = 180°$ corresponds to the bottom.

Inspection of the figures reveals that the largest circumferential variations are those at the first measurement station and that there, the highest heat-transfer coefficients occur at the top of the tube. The topside maxima at this station verify the reattachment/collision model that was discussed in the foregoing. It may also be seen that the largest circumferential variations occur in the 0.75–0.5 range of $\dot{m}_1/\dot{m}$ and that these are definitely larger than the circumferential variation for the $\dot{m}_1/\dot{m} = 0$ case (entire flow entering via the center port). Thus, whereas the latter case serves as an upper bound for the $\overline{Nu}_x$ values at any axial station, it does not bound the $Nu_x(\theta)/\overline{Nu}_x$ variations.

The evolution of the angular distributions with increasing x/D does not follow an elementary pattern, although there is an overall trend toward a decay of the variations. In some cases, the decay is monotonic, in others there is a modest increase in the extent of the variation before decay sets in and in still others there is an inversion of the distribution such that the lowest coefficients are at the top. These behaviors occur because the circumferential motions may exhibit intricate patterns and, in certain cases, may persist to considerable downstream distances.

At $Re = 10000$, the extent of the variations has decayed to the range of $\pm 3\%$ for $x/D \geqslant 12$ for all $\dot{m}_1/\dot{m}$ except $\dot{m}_1/\dot{m} = 0.75$, for which variations in the range of $\pm 8\%$ persist for x/D between 12 and 36. The complete absence of circumferential variations at $x/D = 60$ is worthy of note. At $Re = 30000$, the decay is relatively slow for both $\dot{m}_1/\dot{m} = 0.5$ and 0.75, especially for the latter.

As a final comment, brief mention may be made of the results for $\dot{m}_1/\dot{m} = 1$ (no flow through center port). For the fluid passing through the tee, entering at one side port and exiting the other, the aperture in the upper wall of the tee causes a disturbance which creates circumferential variations, as evidenced in Figs. 5 and 6. These disturbances are, apparently, short lived, since the variations have essentially died away before the second measurement station.

CONCLUDING REMARKS

The present experiments have provided detailed information on the heat-transfer coefficients in a tube situated downstream of a mixing tee. Results were obtained for the circumferential average heat-transfer coefficient at a succession of axial stations and for the circumferential variations of the transfer coefficient at each station.

The axial distributions of the average coefficient for the mixing cases are, for all practical purposes, bounded between the distributions for the two limiting cases of no mixing (respectively with the entire flow entering either via the center port or a side port). Furthermore, the distribution curves are ordered more or less according to the proportions of the two component flows. The lowest coefficients are for the straight throughflow (side port entry—side port exit) and the highest are for the right-angle turning (center port entry—side port exit). The mixing and turning of the flow gives rise to a substantial augmentation of the heat-transfer coefficients compared with those in a conventional thermal entrance region and also substantially elongates the thermal entrance length.

At the higher Reynolds numbers of the experiments (i.e. 20000 and 30000), the circumferential average Nusselt numbers, when normalized by the corresponding fully developed value, are insensitive to Reynolds number for a given mixing proportion. Thus, the results obtained here can be applied to Reynolds numbers higher than those employed in the present experiments. The measured fully developed Nusselt numbers agreed very well with established correlations.

The mixing and turning of the flow also gives rise to circumferential variations of the heat-transfer coefficient, with the largest variations in evidence at the first measurement station. At this station, the highest values of the heat-transfer coefficient consistently occur on the same side of the tube as the center port, and the extent of the variations depends on the proportions of the two component flows. The downstream evolution of the circumferential variations is characterized by an overall tendency toward decay, but in some cases there are overshoots and reversals in the shape of the distribution curves. In most cases, the variations decay to $\pm 3\%$ at 12 diameters downstream of the tee, but residual variations persist at 40–60 diameters in certain situations.

REFERENCES

1. A. F. Mills, Experimental investigation of turbulent heat transfer in the entrance region of a circular conduit, *J. Mech. Engng Sci.* **4**, 63 (1962).
2. M. Hishida, Turbulent heat transfer and temperature distribution in the thermal entrance region of a circular pipe, *Bull. J.S.M.E.* **10**, 113 (1967).
3. B. V. Karlekar and R. M. Desmond, *Engineering Heat Transfer*, p. 351. West Publishing Co., St. Paul (1977).

L'EFFET DU MELANGE PAR UN TE SUR LE TRANSFERT THERMIQUE TURBULENT DANS UN TUBE

Résumé—On détermine expérimentalement les coefficients de transfert pour un écoulement d'air turbulent dans un tube circulaire situé en aval d'un té. Dans les expériences, des écoulements d'air orientés perpandiculairement sont amenés à un té. L'écoulement sortant du té par l'autre côté passe dans la portion de tube chauffée. A partir des résultats obtenus on détermine le coefficient de convection thermique moyen dans des sections droites successives et la variation circonférentielle du coefficient de convection à chaque section. On trouve que le brassage et le changement de direction de l'écoulement provoque une substantielle augmentation des coefficients de convection en comparaison de ceux dans une région d'entrée conventionnelle; la longueur d'établissement thermique est aussi nettement augmentée. Pour un nombre de Reynolds donné, les distributions axiales des coefficients moyens sont bornées par les deux distributions limites de non-mélange (par exemple écoulement total entrant par une seule branche soit latérale soit centrale). Quand les distributions axiales sont normées par les valeurs correspondantes du régime établi, elles sont presque insensibles au nombre de Reynolds. Les variations circonférentielles sont plus grandes juste en aval du té. Dans la plupart des cas, les variations diminuent à $\pm 3\%$ douze diamètres en aval du té, mais quelques fois des variations résiduelles persistent à 40 ou 60 diamètres.

DER EINFLUSS DER MISCHUNG NACH EINEM T-STÜCK AUF DEN TURBULENTEN WÄRMETRANSPORT IN EINEM ROHR

Zusammenfassung—Für turbulente Luftströmung in einem kreisrunden Rohrhinter einem T-Stück wurden die Wärmeübergangskoeffizienten experimentell bestimmt. In den Experimenten waren die Luftströme zueinander senkrecht, d. h. vom zentralen und seitlichen Zweig des T-Stücks wurde zugeströmt. Die sich vereinigende Strömung verläßt das T-Stück durch den anderen seitlichen Zweig und strömt in den beheizten Testabschnitt des Rohres. Aus den experimentellen Daten konnten Werte für über den Umfang gemittelte Wärmeübergangskoeffizienten in axial hintereinanderliegenden Abschnitten und für die periphere Variation der Übergangskoeffizienten dieser Abschnitte ermittelt werden. Das Mischen und Umlenken der Strömung ergab—verglichen mit Werten üblicher Einlaufzonen—eine erhebliche Zunahme des Wärmeübergangskoeffizienten; die thermische Anlauflänge ist ebenfalls größer. Für eine bestimmte Reynolds–Zahl liegt die axiale Verteilung der über den Umfang gemittelten Koeffizienten zwischen den beiden Grenzfällen ohne Mischung, (d. h. einmal tritt die Strömung vom seitlichen und das andere Mal vom zentralen Zweig ein). Bezieht man die axialen Verteilungen auf die Werte bei vollausgebildeter Strömung, so sind sie fast unabhängig von der Reynolds–Zahl. Die größte Variation über dem Umfang findet sich unmittelbar nach dem T-Stück. In den meisten Fällen ist in einer Entfernung von zwölf Durchmessern stromabwärts nach dem T-Stück dieser Variationsbereich auf $\pm 3\%$ abgefallen, aber in einigen Fällen bleibt eine Variation im Abstand von 40 bis 60 Durchmessern noch bestehen.

ВЛИЯНИЕ СМЕШЕНИЯ В Г-ОБРАЗНОМ СМЕСИТЕЛЕ НА ТУРБУЛЕНТНЫЙ ПЕРЕНОС ТЕПЛА В ТРУБЕ

Аннотация — Проведено экспериментальное определение коэффициентов переноса тепла при турбулентном течении воздуха в кольцевой трубе за Г-образным смесителем. Два перпендикулярно направленных друг к другу воздушных потока подавались через центральное и одно боковое отверстие Г-образного смесителя, а смешанный поток истекал из второго бокового отверстия в нагреваемый участок трубы. По полученным экспериментальным данным определены значения среднего тангенциального коэффициента теплопереноса в нескольких поперечных сечениях трубы и его изменение в аксиальном направлении. Найдено, что смешение потока и истечение под углом приводят к существенному увеличению значений коэффициента переноса тепла по сравнению со случаем обычного входного теплового участка. Длина теплового входного участка также значительно увеличивается. При заданном числе Рейнольдса аксиальные распределения тангенциального среднего коэффициента ограничены двумя предельными случаями отсутствия смешения (т. е. когда весь поток подаётся через боковое или через центральное отверстие). При отнесении аксиальных распределений к соответствующим значениям для полностью развитого течения влияние числа Рейнольдса почти исключается. Наибольшие изменения в значениях тангенциального коэффициента теплообмена наблюдаются непосредственно за смесителем. На расстоянии 12 диаметров от смесителя изменения в большинстве случаев затухают в пределах $\pm 3\%$, но в некоторых случаях изменения наблюдаются даже на расстоянии 40–60 диаметров.